accuracy became excessive. Instead, a procedure involving a three-fold application of Simpson's rule was adopted. With this method an accuracy considerably better than 0.1% in the results of the r_1, r_2, r_3 integration could be achieved by subdividing the r_1, r_2 and r_3 ranges of integration into 30, 50 and 30 parts respectively, so that each integration required 49,011 evaluations of the integrand, a process requiring about 121 sec. of computation time. The value of c was taken as 1.0 and the values of c_1, c_2 and c_3 determined by experience. It was found that contributions to the integral in Eq. (A1) were negligible outside a region given by $c_1 = c_3 = 3.0\, y_2$ and $c_2 = 5.0\, y_2$.

Some Experiments with Plumes in a Cross Flow

By I. R. Wood, Ph.D., M.I.E.Aust. and A. M. Grove, M.Eng.Sc., M.I.E.Aust.*

Summary.—This paper reports on some laboratory measurements of plumes in a smooth cross flow. Data are provided which for a cross flow with a low turbulence level, enables the dimensionless trajectory of the plume to be obtained in terms of the flux of density excess, the velocity of the cross wind and the velocity of exit from the plume orifice.

It is noted that the plume observations in the laboratory differ significantly from those in the atmosphere. The differences in the conditions in the laboratory and in the atmosphere are the very low Reynolds number of laboratory plumes and the relatively low turbulence level in the laboratory cross flows. These effects must have caused the difference in the plume trajectories but the manner in which they act is not clear.

LIST OF SYMBOLS

D	Orifice diameter.
F	Flux of density excess or deficit.
g	Acceleration of gravity.
Q	Volume flux from the plume.
U	Ambient fluid velocity.
w	Velocity of the plume at the orifice.
ρ_a	Density of the ambient fluid.
$\Delta\rho$	Plume density excess or deficit.
ν	Kinematic viscosity.

INTRODUCTION

The bending of a plume in a cross wind and the dispersion of the buoyant material in it are frequently observed phenomena. Important examples of this type of flow are the smoke from a chimney, and the dispersion of buoyant sewage in a moving ocean. In both cases it is important to know the manner in which the buoyant material disperses. When the atmosphere surrounding the plume is stationary, there is, apart from a small zone of flow establishment next to the outlet of the chimney, a single region in which the turbulence generated by the buoyancy forces dominates the mixing. In this case it can be shown that the entrainment velocity perpendicular to the plume axis is a constant fraction of the centre-line velocity (Ref. 1), and using the equations of continuity, continuity of buoyant material and momentum, a solution may be obtained. This solution is in reasonable agreement with experimental results.

With a very smooth gentle cross wind, it is possible that the plume will behave in much the same manner as a plume in the absence of a cross wind. That is, the dimensions and velocities of the plume will be much the same as in the absence of the cross wind and the only effect of the moving environment will be to displace the upper regions of the plume away from the vertical line through the axis of the chimney. This type of action was suggested by Priestley (Ref. 2).

With a strong cross wind with a low level of turbulence there are a number of conflicting theories. This is not altogether surprising as there are at least three distinct flow regions (Fig. 3) and the most important mechanism for the generation of turbulence differs in each region.

Close to the flow outlet there is a zone of flow establishment where the potential flow leaving the outlet is sheared. In this region the streamlines within the plume are still almost parallel to those at the outlet. The flow of the ambient fluid around the plume resembles the flow around a cylinder at low Reynolds numbers (Ref. 3) and the shear forces between the ambient fluid and the cylindrical plume section develop two vortices in the plume flow. In this region the production of turbulence is dominated by the shear forces.

Beyond the zone of flow establishment there is a region where a rapid entrainment of the cross flow makes itself apparent by the bending of the plume and the growth of the pair of vortices. This is a relatively short region and in it the plume trajectory has a relatively small radius of curvature and changes from a few degrees from the vertical to an almost constant slope. At the end of this region the effect of the shear forces has become unimportant and the buoyancy force predominates in the generation of turbulence.

Finally, there is a region in which the main effects seem to be those caused by the buoyancy generated turbulence and the slope of the trajectory is almost constant. Even this region is not simple and at least two possible flow regimes may exist.—

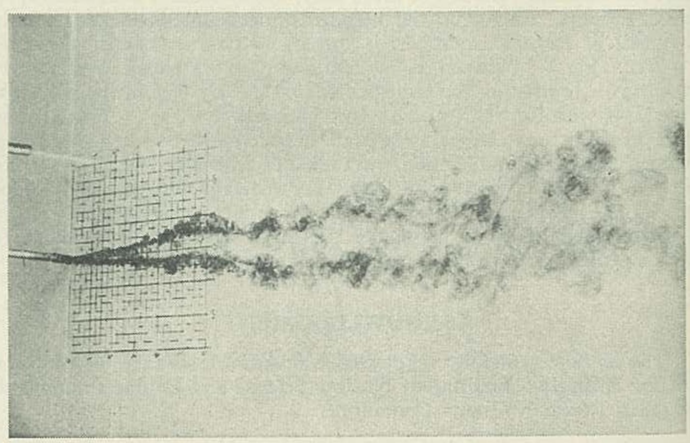

Fig. 1(a).—Plan View of a Split Plume.

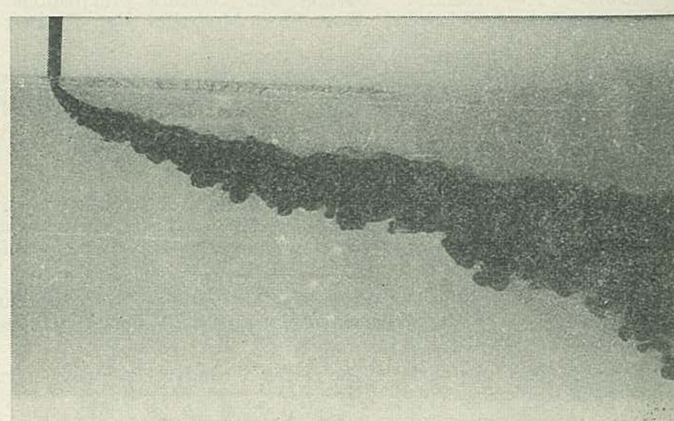

Fig. 1(b).—Elevation View of a Split Plume.

*Paper No. 2562, presented at the Third Australasian Conference on Hydraulics and Fluid Mechanics held at Sydney from 25th to 29th November, 1968.

Dr. Wood is a Senior Lecturer, University of New South Wales, and Mr. Grove is an Engineer, Commonwealth Department of Works, Darwin.

(1) If the cross flow is sufficiently smooth and the flow issuing from the outlet is of a low Reynolds number there is a possibility that the flow may bifurcate as in Figs. 1 (*a*) and 1 (*b*). Fig. 1 (*a*) shows a plume with marked bifurcation. However, when viewed in elevation, the marked three-dimensional effect in these line vortices is apparent (Fig. 1 (*b*)). Indeed small vortex rings of buoyant fluid appear to be falling from the line vortices. Thus the undersurface of the plume is much more irregular than the upper surface. Turner (Ref. 4) has analysed theoretically the motion of these two line vortices.

(2) If the cross flow is relatively turbulent or the eddies induced at the flow outlet have not decayed sufficiently, the plume does not bifurcate. There are still two counter-rotating vortices but there is buoyant fluid between them. A vertical section through the plume at this stage appears very similar to the two-dimensional thermal described by Scorer (Ref. 5), Richards (Ref. 6) and Csanady (Ref. 7). Even when this appears to be the case, an elevation of the plume reveals that the lower surface of the plume is markedly more irregular than the upper surface (Fig. 2) and emphasises the importance of the three-dimensional eddies in the diffusion of the plume.

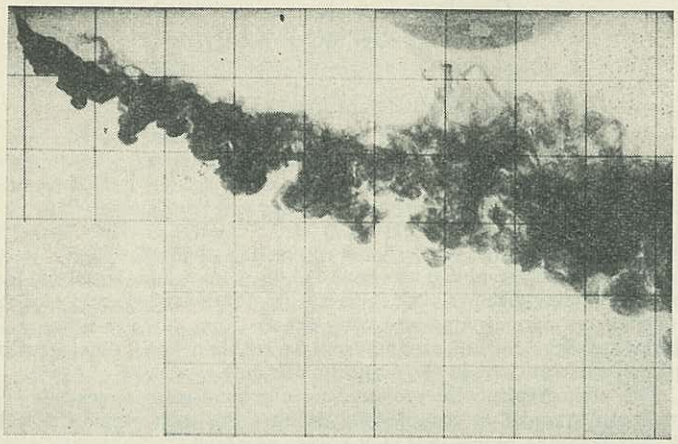

Fig. 2.—Elevation of a Normal Plume.

Indeed, even in the absence of marked turbulence in the cross wind there exists the possibility that at large distances from the chimney the plume may break down into a series of distinct blobs. Each of these blobs would then behave as three-dimensional thermals. This type of flow has been observed in flows from chimneys by Moore (Ref. 8) and Scriven (Ref. 9). The types of flows possible become even more complicated if a range of turbulent intensities is considered in the cross flow. Indeed, the flows described above would all be included in Slawson and Csanady's first phase of plume behaviour (Ref. 10). That is, the phase where self-generated turbulence dominates mixing. Their remaining two phases are the intermediate phase where the environmental turbulence in the inertial subrange dominates the mixing, and the final phase where the energy containing eddies of the environmental turbulence, dominate the mixing.

This study is restricted to plumes of type (2) where the cross wind has a low degree of turbulence but the eddies at the outlet are sufficient to prevent the plume bifurcating. In the region over which the plume was examined the self-generated turbulence was always greater than the turbulence in the surrounding ambient fluid. In spite of these restrictions it is apparent that the behaviour of the plume is extremely complicated.

DIMENSIONAL ANALYSIS

It is appropriate to make the assumption that the variations of the fluid density throughout the flow field are sufficiently small when compared with a reference density (the density of the ambient fluid) that variations of density can be ignored when considering inertia forces. The variations of density are to be included when connected with gravitational terms but it is this Boussinesq assumption which enables flows with a density deficit (a rising plume) to be compared with flows with a density excess (a falling plume).

With this assumption and the variables in Fig. 3, dimensional analysis yields

$$z/D = \phi([x/D], [F/U^3 D], [F/w^3 D], [w D/\nu])$$

where x and z are, respectively, the horizontal and vertical distance from the plume outlet,
D is the diameter of the plume outlet,
F is the flux of density excess or deficit and equals $Q(\Delta\rho\, g/\rho_a)$, where Q is the volume flux from the plume outlet,
ρ_a is the density of the ambient fluid,
$\Delta\rho$ is the plume fluid density excess or deficit at the plume outlet,
g is the acceleration of gravity,
U is the ambient fluid velocity,
w is velocity of the plume fluid at the plume outlet,
ν is the kinematic viscosity assumed the same for the fluid in the plume and in the ambient flow.

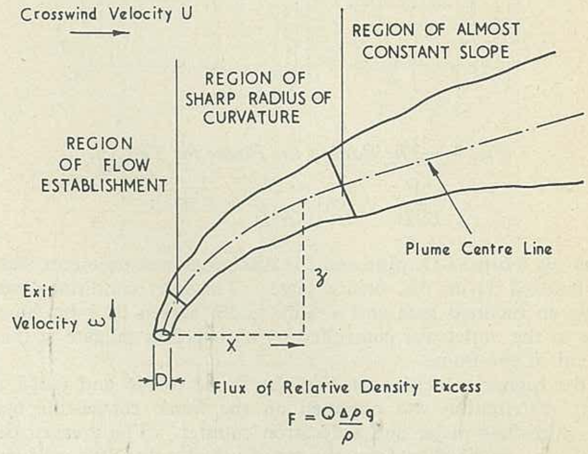

Fig. 3.—Notation.

Now all the plume flows considered are fully turbulent and it is therefore permissible to assume that molecular effects are small compared with those associated with the turbulence. This implies that the Reynolds number may be neglected. Further, in the initial study we will consider the case where the exit velocity from the plume outlet is sufficiently small that for all regions except for a small region near the outlet, the exit momentum is negligible compared to the momentum developed by the buoyancy forces. This implies the neglect of the term $[F/w^3 D]$ and we are left with the following relationship:—

$$z/D = \phi([x/D], [F/U^3 D])$$

To proceed further, it is necessary to assume a knowledge of the manner in which the plume behaves. Once this assumption has been made, the equations of continuity of density deficit and the momentum equation can be used to determine a relationship between the variables. The main assumptions and their implications are set out in Table I.

TABLE I

Assumption	Consequence
(1) The plume is unaffected by the cross wind except in so far as it is sheared over by the wind.	$z/D = K_1 [F/U^3 D]^{1/4} [x/D]^{3/4}$
(2) The plume behaves as a two-dimensional thermal being carried along by the wind.	$z/D = K_2 [F/U^3 D]^{1/3} [x/D]^{2/3}$
(3) The plume breaks up into distinct three-dimensional thermals and these are carried along by the wind.	$z/D = K_3 [F/U^3 D]^{1/4} [x/D]^{1/2}$

In Table I, K_1, K_2 and K_3 are dimensionless constants which depend on the rate of entrainment into the plume and the velocity distribution in the plume. In (2) and (3) laboratory experiments with two-dimensional and axisymmetric thermals (Refs. 6 and 11) have shown that K_2 and K_3 may vary from experiment to experiment in a manner that is not understood. However, as already noted, it appears possible that at least two of the above mechanisms may occur in different degrees simultaneously in one plume. Therefore, at the present state of theoretical knowledge there appears to be little to be gained by further pursuing these theories and dimensional analysis appears to be the only guide to the organisation of experiments.

EXPERIMENTS

The experiments were carried out in a 22-ft. long, 24-in. wide and 14-in. deep flume. Water for the cross flow was supplied from a constant

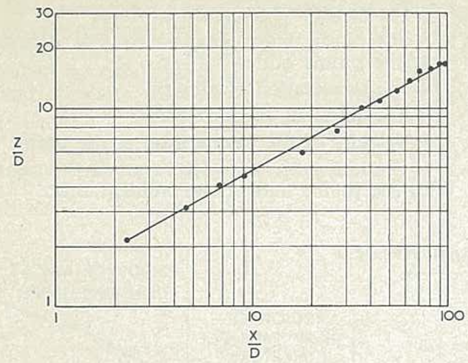

Fig. 4.—The Path of the Plume for Test 15.

$$\frac{F}{U^3D} = 0.61; \frac{F}{w^3D} = 0.67$$

head tank via a 6-in. I.D. pipe and the discharge measurements were made with a standard $3\frac{1}{2}$-in. dia. orifice plate. The inlet conditions were controlled by an inclined gate and a 4-in. width screen of $\frac{3}{4}$ in. blue metal. The flow at the outlet was controlled by an overflow tailgate at the downstream end of the flume.

At the higher velocities used in the flume (0.166 and 0.215 ft./sec.) a velocity distribution was obtained on the flume centre-line using the D.S.I.R. mini-flow meter and a decatron counter. The greatest deviation of the velocity distribution from the mean velocity was 10% and the mean velocity on the centre-line agreed with that calculated from the discharge and the area of the flume to within the experimental error ($\pm$ 3%). The lower velocities used were below the range of the instrument and it was accepted that the mean velocity calculated from the orifice discharge and the area of the flow was a sufficiently accurate measurement of the cross flow velocity.

A dyed solution of sodium chloride was injected at a point 8 ft. downstream of the gravel filter at a height of 1.1 ft. above the channel floor and about 0.10 ft. below the water surface.

The salt solution was supplied from a Mariotte type constant head tank through a 0.25-in. needle valve to a 0.221-in. internal diameter orifice. (This orifice narrowed to 0.161 in. approximately two diameters from the outlet.) This orifice was set in a 1-ft. square, $\frac{1}{8}$-in. thick perspex plate which had a carefully streamlined leading edge and was carefully aligned in the flow. The flat plate was used to remove the effect of the wake of the supply tube. During all the tests the head of salt water in the constant head tank was kept at 0.084 ft. above the level of the ambient fluid and this ensured that the inlet momentum was always small. Discharge rates were determined by timing the fall of water in the Mariotte constant head tank. On the perspex face of the flume was placed a square grid of such a size that when photographed it appeared as a 2-in. grid on the flume centre-line.

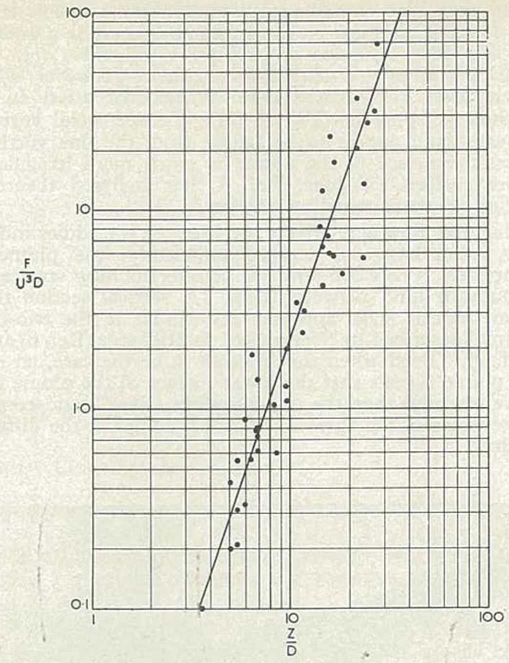

Fig. 5.—$\frac{Z}{D}$ *vs.* $\frac{F}{U^3D}$ *for* $\frac{x}{D} = 18.2; \frac{F}{w^3D} = 0.33.$

The shape of the plume was recorded on 35-mm. film with from three to six shots being taken at each different density deficit. A series of tests was conducted over a range of density deficits from 0.5% to 9.5% at five different ambient velocities ranging from 0.5 to 2.0 in./sec. Photographing of the plumes was done in the vertical plane only.

The photographs were projected on a ground-glass screen and were plotted and averaged at each density deficit. For each plume the values of x and z on the plume centre-line were recorded.

ANALYSIS

In the experiments the trajectory and the mean widths of the plumes were obtained for a 700-fold range of $[F/U^3 D]$ (from 0.09 to 69.4) while the restriction maintained on the momentum inflow kept the variation of $[F/w^3 D]$ to a 25-times range (from 0.04 to 1.0). It was therefore considered reasonable to ignore the variation in $[F/w^3 D]$ in the first analysis.

Initially values of $\log[z/D]$ were plotted against $\log[x/D]$ for constant $[F/U^3 D]$ and against $\log[F/U^3 D]$ for a constant $[x/D]$ (Figs. 4 and 5). Once it was apparent that straight lines would fit all the plotted data with reasonable accuracy, the data were punched onto cards and the lines of

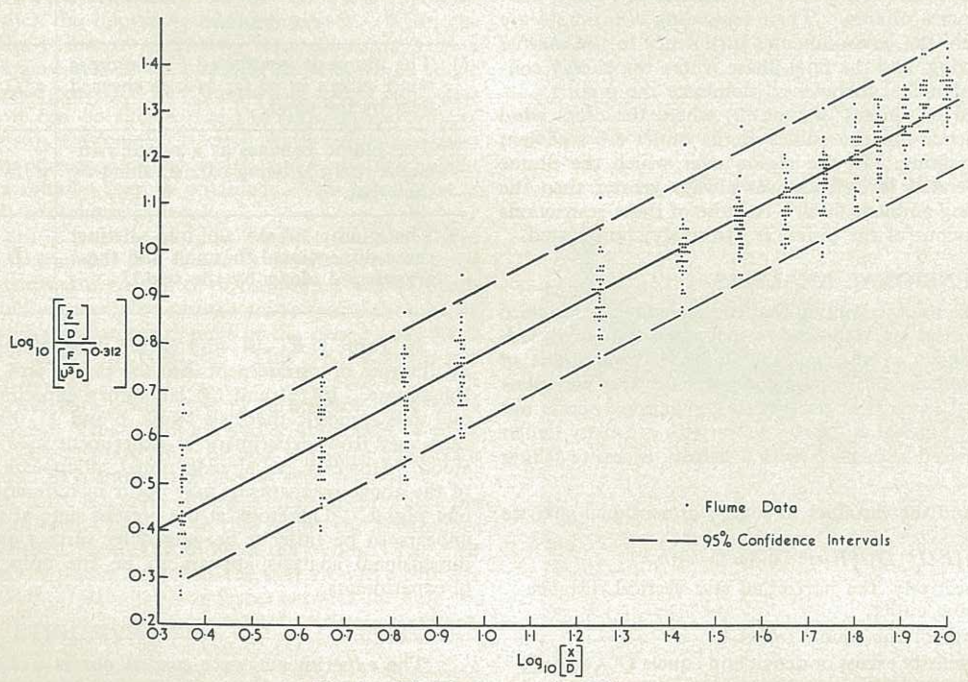

Fig. 6.—The Trajectory of a Plume.

best fit were obtained using linear regression analysis. The mean slope of the 14 plots of $\log[z/D]$ *versus* $\log[F/U^3 D]$ (for a constant x/D) was found to be 0.312 with a standard deviation of 0.026. Similarly the mean slope of the $\log[z/D]$ *versus* $\log[x/D]$ (for a constant $[F/U^3 D]$) for the 41 test runs was 0.537 with a standard deviation of 0.07.

The standard deviation of the first plots was considerably less than that in the second and it was therefore decided to plot $\log([z/D]/[F/U^3 D]^{0.312})$ *versus* $\log[x/D]$ as shown in Fig. 6. The line of best fit has a slope of 0.529 and is defined by the equation

$$\log[z/D] - 0.312 \log[F/U^3 D] = 0.249 + 0.531 \log[x/D]$$

There is a considerable scatter of the test results about this line and the 95% confidence limits (Ref. 12) have been computed as shown in Fig. 6.

Finally, an attempt was made to sort out the deviation from this line

$$\log[z/D] - 0.312 \log[F/U^3 D] = 0.249 + 0.531 \log[x/D]$$

with the term $[F/w^3 D]$. This term was obviously important at small values of $[x/D]$ but relatively unimportant at large distances from the source. However, the scatter in the points tended to hide any trend. This was not entirely unexpected as the plume itself was extremely variable and the variation in $[F/w^3 D]$ had deliberately been kept as small as possible.

DISCUSSION OF THE RESULTS

It is apparent that the experimental points fit the equation

$$z/D = 1.77\,[x/D]^{0.53}\,[F/U^3 D]^{0.312}$$

and that this does not support any of the proposed hypotheses. Indeed it appears that the plume behaves as something between the two-dimensional line thermal and a series of discrete three-dimensional thermals.

It is appropriate at this stage to compare these experimental results with other published work. Fan (Ref. 13) has recently carried out a number of experiments similar to but more detailed than the authors'. He analysed the results in a completely different manner and used a different arrangement of variables in his dimensionless terms. However, his data show that he varied the values of $[F/U^3 D]$ from 0.03 to 4.0 and $[F/w^3 D]$ from 0.00015 to 0.0075. It is apparent that no attempt was made to maintain the inflow momentum small, and his study deals with forced plumes (i.e., plumes in which the initial momentum cannot be ignored). Further, he measured his trajectories by measuring the concentrations along the vertical central plane of the plume and determining the $[z/D]$ of the position of the maximum concentration. However, sufficient traces are published so that trajectories based on the centre-line between the edges of the dyed salt solution can be obtained. With these data it is possible to check the conclusions obtained from the authors' experiments. Fig. 7 shows that for a constant $[F/w^3 D]$ of 0.0005 and at $[x/D]$ values of 30 and 90 the variation of $[z/D]$ with $[F/U^3 D]$ obtained from the authors' experiments, is still satisfactory. The values of $\log([z/D]/[F/U^3 D]^{0.312})$ obtained from Fan's experiments were then averaged at values of $[F/w^3 D]$ and $[x/D]$ and are plotted against $\log[x/D]$ in Fig. 8.

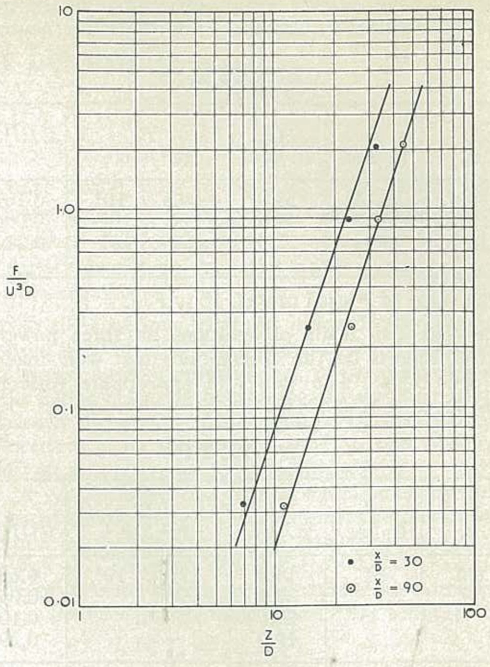

Fig. 7.— $\frac{Z}{D}$ *vs.* $\frac{F}{U^3D}$ *for* $\frac{x}{D} = 30$ *and* 90; $\frac{F}{w^3D} = 0.0005$.
Data from Fan (Ref. 13).

This Fig. 8 then gives a reasonably complete picture of the trajectory of plumes released with varying quantities of initial momentum in the uniform cross stream of laboratory flumes. In these flumes the turbulence level will be relatively low. Fan suggests that this level was under 5% in his channel and carried out some check experiments with the orifice towed in a stationary fluid. The results from these experiments were indistinguishable from those carried out in the moving ambient fluid.

ATMOSPHERIC OBSERVATIONS

It is of considerable interest to compare the results obtained in laboratory channels with measurements made in the atmosphere. Slawson and

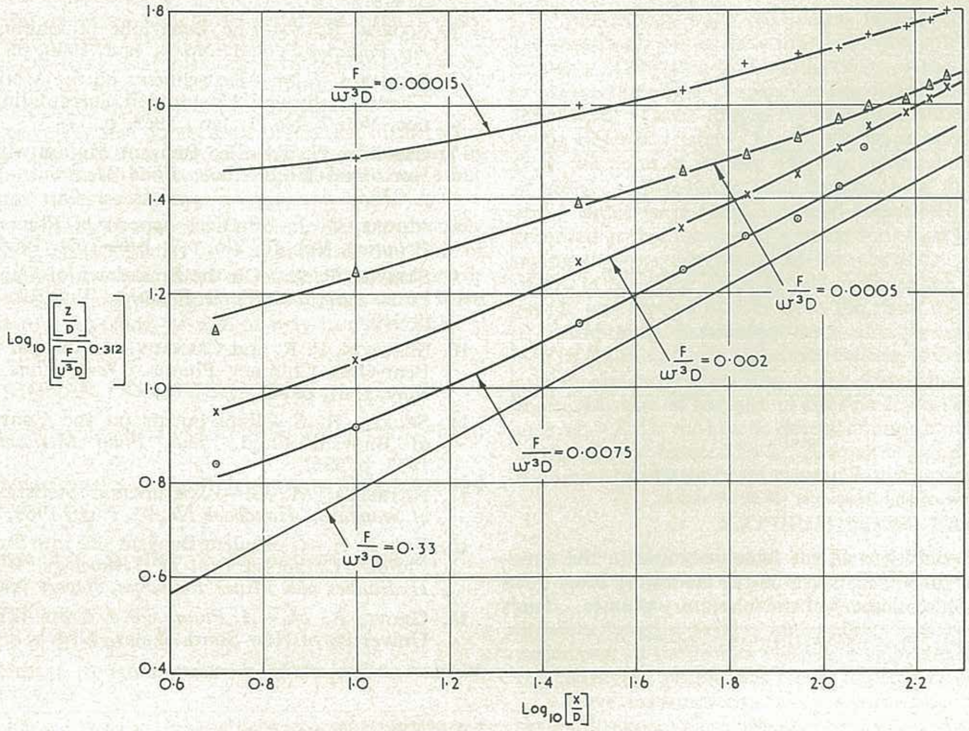

Fig. 8.—The Trajectory of Force Plumes.
Data from Fan and Grove (Refs. 13 and 14).

Csanady (Ref. 10) have recently made observations of the trajectory of a plume from a power plant in Canada. The values for neutral conditions are listed in Table II.

TABLE II

Plume	D ft.	w ft./sec.	U ft./sec.	F ft.^{4}/sec.^{3}	F/U^3D	F/w^3D
E_1	19.5	30.4	33.0	89.5×10^3	0.167	0.127
E_3	19.5	67.0	49.0	220×10^3	0.096	0.035
E_7	19.5	66.2	38.0	226×10^3	0.210	0.039

Note: The value of F used in Ref. 10 is F/π.

Bosanquet has also made observations on three power plants and Priestley (Ref. 2) reports on the observations that were made for neutral atmospheric conditions. The values of appropriate variables for these conditions are listed in Table III.

TABLE III

Plant No.	D ft.	w ft./sec.	U ft./sec.	F ft.^{4}/sec.^{3}	F/U^3D	F/w^3D
1	6.4	31	14.0	12.1×10^3	0.69	0.063
			33.0	,,	0.055	0.063
			26.5	,,	0.10	0.063
			19.0	,,	0.29	0.063
2	3.9	28	10.0	8.6×10^2	0.22	0.0105
			13.3	,,	0.09	0.0105
3	6.5	35.5	20.4	13.4×10^3	0.24	0.061

The values of $[F/U^3D]$ in these observations were in the range of values of $[F/w^3D]$ where in the flume experiments the effects of variations of $[F/w^3D]$ on the trajectory were small (Fig. 8). The variation of $[F/w^3D]$ was therefore ignored and the published data were plotted in the same manner as the flume experiments (Fig. 9). A straight line could reasonably be fitted through the plot of $\log([z/D]/[F/U^3D]^{0.312})$ *versus* $\log[x/D]$ but this line

$$[z/D] = 1.71\,[F/U^3D]^{0.312}\,[x/D]^{0.66}*$$

had a slope that was considerably greater than that obtained from the flume experiments.

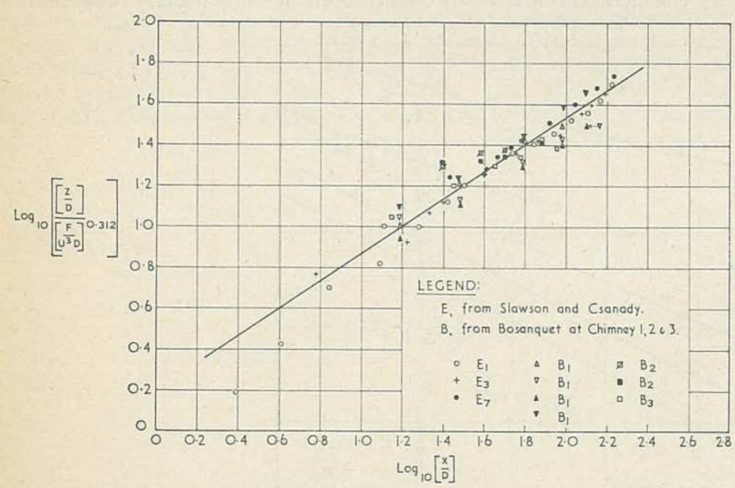

Fig. 9.—The Trajectory of Plumes in the Atmosphere.
Data from Slawson and Bosanquet (Refs. 10 and 2).

The differences in the conditions in the laboratory and in the atmosphere are the relatively low turbulence levels in the laboratory cross flows and the relatively low Reynolds numbers of the laboratory plumes. Fan's plumes had outlet Reynolds numbers of from 8 to 18,000. The authors' outlet Reynolds numbers were in the laminar flow range but it is believed that the large step close to the outlet provided large eddies in the flow and that the flow became fully turbulent almost immediately after leaving the nozzle. The manner in which these effects change the trajectory is not clear.

*Csanady's expression reduces to $[z/D] = 1.56\,[F/U^3D]^{0.333}\,[x/D]^{0.666}$.

CONCLUSIONS

The significant conclusions from this series of experiments are:

(1) the trajectory of a plume of buoyant material released in cross flow with a low turbulence level may be obtained from Fig. 8. It is believed that this may be useful in predicting the path of a buoyant pollutant in a moving environment such as the ocean.

(2) Observations in the atmosphere suggest that although the variation of the plume trajectory with $[F/U^3D]$ is much the same as that obtained in laboratory flumes, the slope of the trajectory of the plume is greater in the atmosphere, than that obtained in the laboratory. For " large " values of $[F/w^3D]$ (i.e., relatively small values of the inflowing momentum) we obtain in the laboratory

$$Z/D = 1.77\,[F/U^3D]^{0.312}\,[x/D]^{0.53}$$

and in the atmosphere

$$z/D = 1.71\,[F/U^3D]^{0.312}\,[x/D]^{0.66}$$

ACKNOWLEDGMENTS

The experimental work and a preliminary analysis of the data were carried out by Mr. A. M. Grove as a post-graduate student under the supervision of Dr. I. R. Wood.

The authors would like to acknowledge the assistance of the staff of the Water Research Laboratory in the development of this paper and to thank Mr. D. Watts for permission to reproduce the photographs of a split plume.

References

1. MORTON, B. R., TAYLOR, *Sir* Geoffrey and TURNER, J. S.—Turbulent Gravitational Convection from Maintained and Instantaneous Sources. *Proc. Roy. Soc., Series A*, Vol. 234, No. 1196, Jan. 24, 1956, pp. 1-23.
2. PRIESTLEY, C. H. B.—A Working Theory of the Bent-Over Plume of Hot Gas. *Quarterly Jour. Roy. Meteorological Soc.*, Vol. 82, No. 352, April, 1956, p. 165.
3. PRATTE, B. D. and BAINES, W. D.—Profiles of the Round Turbulent Jet in a Cross Flow. *Proc. A.S.C.E. Jour. Hydraulics Div.*, Vol. 93, No. HY6, Nov., 1967, p. 53 (Paper No. 5556).
4. TURNER, J. S.—A Comparison between Buoyant Vortex Rings and Vortex Pairs. *Jour. Fluid Mechanics*, Vol. 7, Pt. 3, March, 1960, p. 419.
5. SCORER, R. S.—The Behaviour of Chimney Plumes. *Int. Jour. of Air Pollution*, Vol. 1, No. 3, Jan., 1959, p. 198.
6. RICHARDS, J. M.—Experiments on the Motions of Isolated Cylindrical Thermals through Unstratified Surroundings. *Air and Water Pollution*, Vol. 7, No. 1, Jan., 1963, p. 17.
7. CSANADY, G. T.—The Buoyant Motion within a Hot Gas Plume in a Horizontal Wind. *Jour. Fluid Mechanics*, Vol. 22, Pt. 2, June, 1965, p. 225.
8. MOORE, D. J.—Physical Aspects of Plume Models. *Air and Water Pollution*, Vol. 10, No. 6-7, June-July, 1966, p. 411.
9. SCRIVEN, R. A.—On the Breakdown of Chimney Plumes into Discrete Puffs. *Air and Water Pollution*, Vol. 10, No. 6-7, June-July, 1966, p. 419.
10. SLAWSON, P. R. and CSANADY, G. T.—On the Mean Path of Buoyant Bent-Over Chimney Plumes. *Jour. Fluid Mechnics*, Vol. 28, Pt. 2, May, 1967, p. 311.
11. SCORER, R. S.—Experiments on the Convection of Isolated Masses of Buoyant Fluid. *Jour. Fluid Mechanics*, Vol. 2, Pt. 6, Aug., 1957, p. 583.
12. NATRELLA, M. G.—Experimental Statistics. *U.S. National Bureau of Standards, Handbook No.* 91, Aug., 1963, Chapter 5, p. 5-11.
13. FAN, L. N.—Turbulent Buoyant Jets into Stratified or Flowing Ambient Fluids. *California Inst. of Technology, W. M. Keck Laboratory for Hydraulics and Water Resources, Report No.* KH-R-15, June, 1967.
14. GROVE, A. M.—*A Plume in a Cross Wind.* Thesis (M.Eng.Sc.), University of New South Wales, 1966.